Progress In Electromagnetics Research, Vol. 135, 515–525, 2013

DESIGN OF COMPACT DUAL-BAND FILTER IN MULTILAYER LTCC WITH CROSS COUPLING

Chunxia Zhou[1, *], Yongxin Guo[2], Lei Wang[1, 2], and Wen Wu[1]

[1]Ministerial Key Laboratory of JGMT, Nanjing University of Science and Technology, Nanjing 210094, China

[2]Department of Electrical and Computer Engineering, National University of Singapore, Singapore 117576, Singapore

Abstract—A very compact low temperature co-fired ceramic (LTCC) dual-band filter is designed based on the proposed novel cross-coupling structure in this paper. A six-pole dual-band filter with four transmission zeros is synthesized using an analytical procedure. By incorporating the proposed novel cross-coupling structure and analyzing the coupling characteristic, the dual-band filter is realized with canonical topology in multilayer LTCC. It is demonstrated by the simulation and experiment that the proposed dual-band filter has both compact size and good selectivity.

1. INTRODUCTION

Filters with multiple passbands and high selectivity are required due to the demand for efficient utilization of more and more frequency channels in modern satellite systems. A dual-mode canonical waveguide filter with dual-passband is presented in [1], but with large size, heavy weight and high cost. A triple-passband Chebyshev filter and a dual-passband quasi-elliptic filter on the basis of substrate integrated waveguide (SIW) technology were demonstrated in [2]. A compact SIW filter was presented in [3] with the type of evanesced-mode, while [4] presented the design method of a type of in-line-pseudo-elliptic SIW filters. These filters usually occupy a large circuit area because of the planar arrangement of the resonators. As multimedia satellite communication requires components with low

Received 23 October 2012, Accepted 21 December 2012, Scheduled 28 December 2012

* Corresponding author: Chunxia Zhou (zhouchx1010@gmail.com).

weight, small size and high reliability, multilayer low-temperature co-fired ceramic (LTCC) technology has been considered as an attractive solution [5–15]. LTCC band-pass filters were introduced in [5–9] while dual band filters implemented in LTCC technology were proposed in [10, 11]. Design approaches for realizing very compact and low-profile unbalanced LTCC filters were presented in [12]. Antennas were also envisaged in this technology, a Bluetooth antenna being implemented in LTCC technology [13]. Support vector regression (SVR) method for LTCC multilayer interconnect modeling was introduced also in [14]. Finally, a LTCC receiver front-end module integrating 9 building blocks was proposed in [15].

In this paper, a dual-band filter with compact size and high frequency selectivity is developed with the multilayer LTCC technology for satellite application. In [2], a structure including a magnetic coupling post-wall iris and a balanced line with a pair of metalized via-holes is placed between SIW resonators to realize the electric coupling. However, it is not suitable for multilayer LTCC technology as the ground etched structure will have effects on other resonators. A novel cross-coupling architecture is proposed for the realization of canonical type dual-band filter on multilayer LTCC. It is realized by two etched slots in the top metal layer of two coupled resonators. Two passbands from 19.0–19.7 GHz and 20.4–21.1 GHz are obtained with four transmission zeros resulting from the proposed novel cross coupling structure. The whole size of the filter is $9.8 \times 4.35 \times 0.576\,\text{mm}^3$.

2. FILTER DESIGN

2.1. Circuit Synthesis

The dual-band filter is synthesized by the following two steps. Firstly, an analytical procedure [16] is used to determine the poles and zeros of the transfer function of the dual-band filter. The procedure for finding the equal-ripple response starts with the initial guess of a set of poles and zeros in each frequency band. The values of transmission zeros and poles are updated to have an equal-ripple performance in each passband and stopband. Poles and zeros of the six-pole dual-band filter with in-band return loss of 20 dB are determined to be $S_{p1} = -j0.9131$, $S_{p2} = -j0.6466$, $S_{p3} = -j0.3873$, $S_{p4} = j0.3873$, $S_{p5} = j0.6466$, $S_{p6} = j0.9131$; $Z_{p1} = -j1.4916$, $Z_{p2} = -j0.6837$, $Z_{p3} = j0.6837$, $Z_{p4} = j1.4916$. Then generalized coupling matrix of the low-pass prototype circuit can be obtained by method described

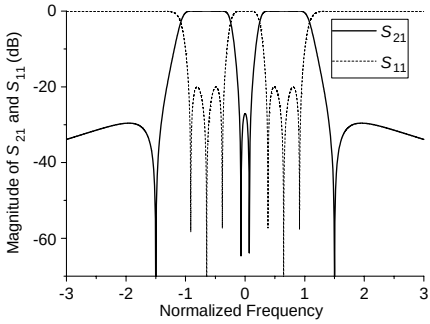

Figure 1. Synthesized S parameters of the dual-band filter.

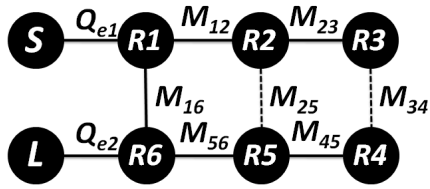

Figure 2. Coupling schematic of the dual-band filter.

in [17]:

$$M = \begin{bmatrix} 0 & 0.7776 & 0 & 0 & 0 & 0.1545 \\ 0.7776 & 0 & 0.3859 & 0 & -0.4197 & 0 \\ 0 & 0.3859 & 0 & -0.3728 & 0 & 0 \\ 0 & 0 & -0.3728 & 0 & 0.3859 & 0 \\ 0 & -0.4197 & 0 & 0.3859 & 0 & 0.7776 \\ 0.1545 & 0 & 0 & 0 & 0.7776 & 0 \end{bmatrix} \quad (1)$$

$R_1 = R_2 = 0.6686$

The synthesized S parameters of the dualband filter are shown in Fig. 1. After the coupling matrix is obtained, a corresponding coupling schematic is built in Fig. 2, where the dashed lines and solid lines mean opposite coupling characteristics.

2.2. Coupling Structure

2.2.1. LTCC Cavity Resonator

The cavity resonator is formed by LTCC substrate with metal outer surfaces and via arrays as vertical sidewalls, which is shown in Fig. 3. The resonator has a length of L and a width of W. Each via has a diameter of d and is separated from its neighboring by a center-to-center spacing s. The resonance frequency of the TE_{110} dominant mode can be determined [18].

$$f_0 = \frac{c_0}{2\sqrt{\varepsilon_r}} \sqrt{\frac{1}{W_{eff}^2} + \frac{1}{L_{eff}^2}} \quad (2)$$

where

$$W_{eff} = W - \frac{d^2}{0.95s}$$
$$L_{eff} = L - \frac{d^2}{0.95s}$$

c_0 is the light velocity in vacuum and ε_r the relative permittivity of LTCC substrate.

2.2.2. External Coupling with CPW Feeding

The filter is excited by 50-Ω CPW structure. The external quality factor is analyzed based on TE_{110} SIW cavity resonator with 50-Ω CPW as its input/output. The coupling is controlled by the length l_p of the coupling slot with a fixed coupling slot width and a fixed post-wall iris width. Fig. 4 shows the calculated Q_e dependent on the length of l_p [19].

2.2.3. Electric Coupling in Different Layer by Rectangular Aperture

To efficiently couple two adjacent cavities in different layers, a rectangular aperture can be placed at the center of two cavities. The coupling coefficient can then be extracted by using the following relation [19]:

$$k = \pm \frac{f_2^2 - f_1^2}{f_2^2 + f_1^2} \tag{3}$$

where f_2 and f_1 stand for the high and low resonant frequencies of the two coupled resonators, respectively.

As the electric field is a maximum in the center of the cavity, the electric coupling can be achieved with this coupling structure, where we can define k as positive. Fig. 5 shows the relationship between the

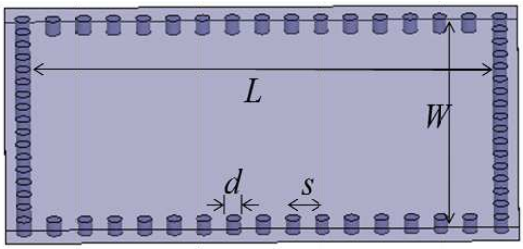

Figure 3. LTCC cavity resonator.

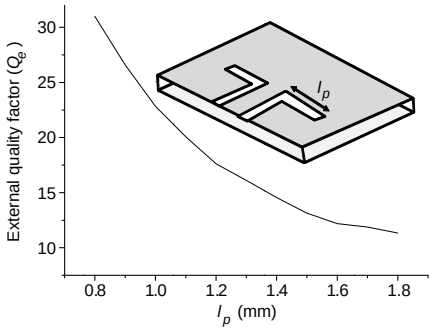

Figure 4. Relationship between the external quality factor Q_e and the length of l_p.

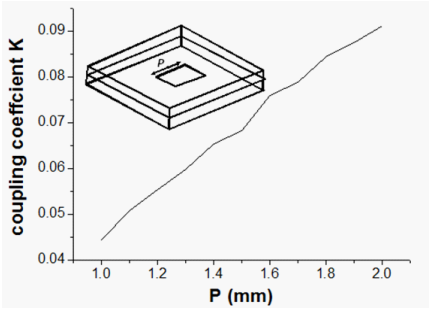

Figure 5. Relationship between the coupling coefficient k and the length P of aperture.

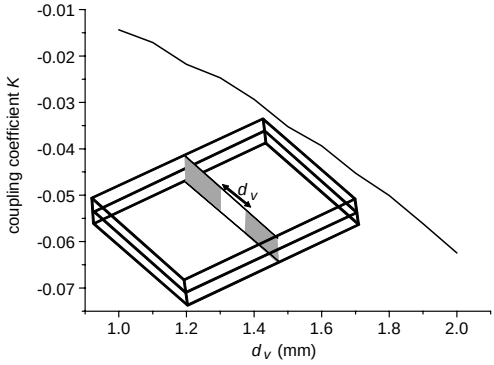

Figure 6. Relationship between the coupling coefficient k and the via distance d_v.

coupling coefficient k and the aperture length P The main couplings M_{12}, M_{23}, M_{45} and M_{56} in Fig. 2 are realized with this structure.

2.2.4. Magnetic Coupling in the Same Layer by Inductive Iris

The inductive window composing of vias are used to control the coupling of the cavities at the same layer. The coupling strength is controlled by the separation of the vias. The wider the separation, the stronger the coupling can be. As the magnetic field has a maximum around the cavity wall, the magnetic coupling can be achieved which can be defined as negative. Fig. 6 shows the relationship between the coupling coefficient k and the via distance d_v The main coupling M_{34} and the cross coupling M_{25} in Fig. 2 are realized with this structure.

2.2.5. Electric Coupling in the Same Layer by the Proposed Novel Structure

As indicated in Fig. 2, electric coupling in the same layer is needed. In [2], a structure including a magnetic coupling post-wall iris and a balanced line with a pair of metalized via-holes is placed between SIW resonators to realize the electric coupling. However, it is not suitable for multilayer LTCC technology as the ground etched structure will have effects on other resonators. A novel coupling structure in multilayer LTCC is proposed in this paper. It is realized by two etched slots in the top metal layer of two coupled resonators, shown in Fig. 7. If we replace the symmetry plan of the coupled resonators with an electric boundary, we can get f_e, that is resonator frequency with electronic wall. If with a magnetic boundary, we can get f_m, which is resonator frequency with magnetic wall. As mentioned in [19], if the frequency shifts of f_e or f_m with respect to their individual uncoupled resonant frequencies are in the same direction, the resultant coupling coefficients will have the same signs, if not the opposite signs. We can

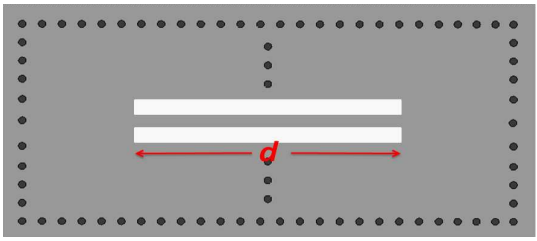

Figure 7. The structure of the proposed novel coupling structure.

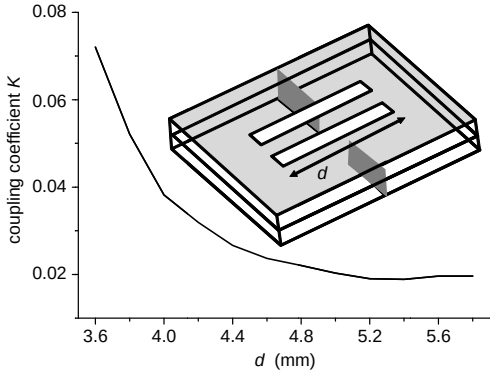

Figure 8. Relationship between the coupling coefficient K as function of d.

find that the frequency shifts of f_e in the proposed structure is in the same direction with the case of the electric coupling in different layer by rectangular aperture. Thus, we can achieve electric coupling through the proposed novel structure. Fig. 8 gives the coupling coefficient K_e as function of d. The novel coupling structure in this paper has etches only in the top metal of the SIW structure, which can be implemented in multilayer LTCC to realize electric coupling. The cross coupling M_{16} in Fig. 2 is realized with this structure.

2.3. Filter Design in LTCC

The configuration of the six-pole dual-band filter in LTCC is shown in Fig. 9(a). The cavity resonators 1 and 6 locate in layer 1, the resonators 2 and 5 locate in layer 2 and the resonators 3 and 4 locate in layer 3. The main couplings M_{12}, M_{23}, M_{45} and M_{56} are realized by rectangular apertures in the common metal layers with the vertical structure, which is electric coupling. The mail coupling M_{34} and the cross coupling M_{25} are realized by inductive irises in the same layer, which are magnetic coupling. According to the synthesized matrix, we need electric coupling for M_{16}, which cannot be realized just by the inductive irises. We proposed a novel cross-coupling structure as analyzed in Section 2.2 to realize M_{16}. Each metal layer and via positions are shown in Figs. 9(b) to (e). After optimization in ansoft HFSS [20], we can get the critical designed parameters: $l_1 = l_6 = 4.89\,\text{mm}$; $l_2 = l_5 = 4.95\,\text{mm}$; $l_3 = l_4 = 4.92$ mm; $l_p = 3.09\,\text{mm}$; $d = 5.5\,\text{mm}$; $d_{12} = d_{56} = 1.85\,\text{mm}$; $d_{23} = d_{45} = 1.4\,\text{mm}$; $d_{34} = 1.6\,\text{mm}$; $d_{16} = 2.75\,\text{mm}$; $d_{25} = 1.65\,\text{mm}$.

3. EXPERIMENT RESULTS AND DISCUSSION

The dual-band filter was fabricated by LTCC technology on the substrate with relative dielectric constant 5.9 and loss tangent 0.002. The thickness of each layer is 0.192 mm. A photo-graph of this filter is shown in Fig. 10. Furthermore, the proposed filter exhibits a size of $1.29\lambda_g \times 0.57\lambda_g$, where λ_g is the wavelength of a 50-Ω microstrip line at the centre frequency. Fig. 11 shows the simulated and measured responses of the filter. A dual-band filter from 19.0–19.7 GHz and 20.4–21.1 GHz with good out-of-band rejection can be achieved. A pair of transmission zeros are observed at 18.5 GHz and 22.5 GHz and another pair of transmission zeros are produced in the stopband. The measure in-band insertion and return loss are better than 2.4 dB and 11.2 dB, respectively.

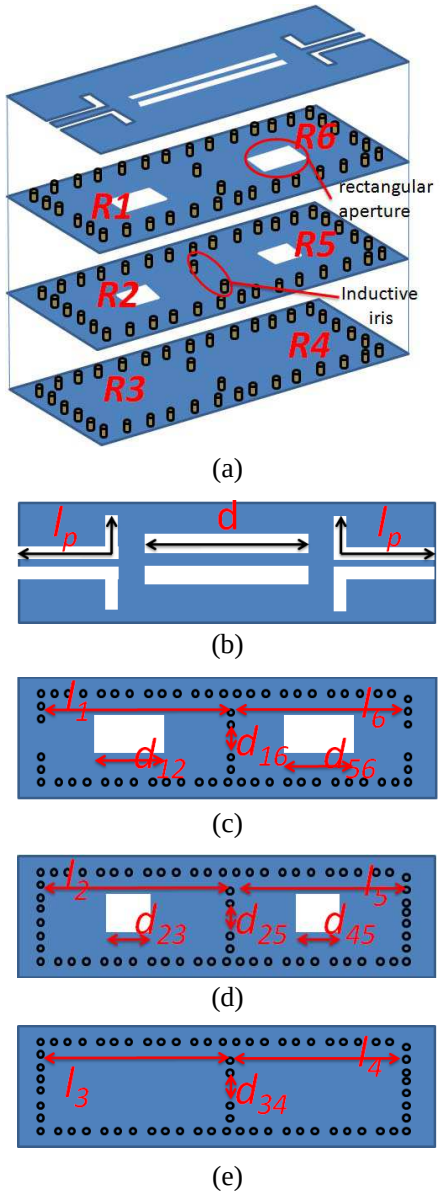

Figure 9. The geometry of the dual-band filter. (a) 3D configuration. (b) Layer 1. (c) Layer 2. (d) Layer 3. (e) Layer 4.

Table 1 shows the performance comparison of the proposed dual-band filter with some published single-band and dual-band LTCC filters. The insertion loss of the proposed LTCC filter is smaller and

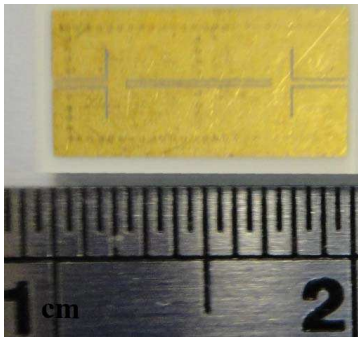

Figure 10. Photo of the fabricated LTCC filter.

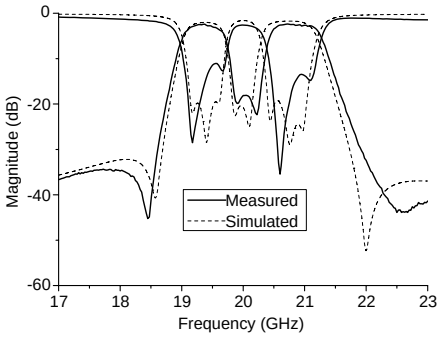

Figure 11. Simulated and measured S parameters of the dual-band filter.

Table 1. Comparison of similar LTCC filters.

Ref.		Order	Insertion loss	Circuit size
[6]	Single-band	3	5 dB	$5\lambda_g \times 2\lambda_g$
[7]	Single-band	4	3.2 dB	$0.57\lambda_g \times 0.56\lambda_g$
[8]	Single-band	2	2.09 dB	$1.27\lambda_g \times 0.71\lambda_g$
[9]	Single-band	4	2.4 dB	$1.44\lambda_g \times 0.79\lambda_g$
[10] 1st	Dual-band	3	4.5 dB	$1.12\lambda_g \times 0.9\lambda_g$
[10] 2nd	Dual-band	4	4.8 dB	$0.93\lambda_g \times 0.88\lambda_g$
This work	Dual-band	6	2.4 dB	$1.29\lambda_g \times 0.57\lambda_g$

the size is comparable to those in [7] and [10]. The proposed filter has two passbands, while with the insertion loss and size comparable to those in [8] and [9].

4. CONCLUSION

This paper has described design method of a dual-band canonical filter in LTCC for satellite application. By incorporating the proposed novel cross-coupling structure, the dual-band filter is designed and fabricated with multilayer LTCC technology. It has been found theoretically and experimentally that the proposed filters have very good selectivity, low insertion loss and compact size.

REFERENCES

1. Lee, J., M. S. Uhmand, and I. B. Yom, "A dual-passband filter of canonical structure for satellite applications," *IEEE Microwave Wireless Components Letters*, Vol. 14, 271–273, 2004.
2. Chen, X.-P., K. Wu, and Z. L. Li, "Dual-band and triple-band substrate integrated waveguide filters with Chebyshev and quasi-elliptic responses," *IEEE Transaction on Microwave Theory and Techniques*, Vol. 5, 2569–2578, 2007.
3. Zhang, Q.-L., W.-Y. Yin, S. He, and L.-S. Wu, "Evanescent-mode substrate integrated waveguide (SIW) filters implemented with complimentary split ring resonators," *Progress In Electromagnetics Research*, Vol. 111, 419–432, 2011.
4. Jedrzejewski, A., N. Leszczynska, L. Szydlowski, and M. Mrozowski, "Zero-pole approach to computer aided design of in-line SIW filters with transmission zeros," *Progress In Electromagnetics Research*, Vol. 131, 517–533, 2012.
5. Xu, L.-J., J. P. Wang, Y.-X. Guo, and W. Wu, "Double-folded substrate integrated waveguide band-pass filter with transmission zeros in LTCC," *Journal of Electromagnetic Waves and Applications*, Vol. 27, No. 1, 1–8, 2012.
6. Wang, Z., X. Zeng, and B. Yan, "A millimeter-wave *E*-plane band-pass filter using multilayer low temperature co-fired ceramic (LTCC) technology," *Journal of Electromagnetic Waves and Applications*, Vol. 24, No. 1, 71–79, 2010.
7. Chin, K. S., C. H. Chen, and C. C. Chang, "LTCC vertically-stacked cross-coupled band-pass filter for LMDS band application," *Progress In Electromagnetics Research C*, Vol. 22, 123–135, 2011.
8. Xu, Z.-Q., Y. Shi, B. C. Yang, P. Wang, and Z. Tian, "Compact second-order LTCC substrate integrated waveguide filter with two transmission zeros," *Journal of Electromagnetic Waves and Applications*, Vol. 26, Nos. 5–6, 795–805, 2012.
9. Xu, M. J., Z. Q. Xu, K. Chen, B. Fu, and J. X. Liao, "Multilayer substrate integrated hexagonal cavity (SIHC) filter with mixed coupling (MC)," *Journal of Electromagnetic Waves and Applications*, Vol. 27, No. 2, 1–9, 2012.
10. Chen, B. J., T. M. Shen, and R. B. Wu, "Dual-band vertically stacked laminated waveguide filter design in LTCC technology," *IEEE Transaction on Microwave Theory and Techniques*, Vol. 57, 1554–1562, 2009.
11. Zhou, C. X., Y. X. Guo, and S. L. Yan, "Dual-band UWB filter

with LTCC technology," *Electronics Letters*, Vol. 47, No. 22, 1230–1232, 2011.

12. Tamura, M., T. Yang, and T. Itoh, "Very compact and low-profile LTCC unbalanced to balanced filters with hybrid resonators," *IEEE Transaction on Microwave Theory and Techniques*, Vol. 59, 1925–1936, 2011.
13. Wu, C. Y., K. S. Zheng, and J. Y. Li, "A chip antenna in via-free LTCC with symmetric structure for Bluetooth applications," *Journal of Electromagnetic Waves and Applications*, Vol. 26, No. 10, 1350–1357, 2012.
14. Xia, L., R. M. Xu, and B. Yan, "LTCC interconnect modeling by support vector regression," *Progress In Electromagnetics Research*, Vol. 69, 67–75, 2007.
15. Wang, Z., P. Li, and R. Xu, "A compact X-band receiver front-end module based on low temperature co-fired ceramic technology," *Progress In Electromagnetics Research*, Vol. 92, 167–180, 2009.
16. Zhang, Y. and K. A. Zaki, "Analytical synthesis of generalized multi-band microwave filters," *IEEE/MTT-S International Microwave Symposium*, 870–876, Honolulu, HI, Jun. 2007.
17. Cameron, R. J., "General coupling matrix synthesis methods for Chebyshev filtering functions," *IEEE Transaction on Microwave Theory and Techniques*, Vol. 47, 433–442, 1999.
18. Cassivi, Y., L. Perregrini, P. Arcioni, M. Bressan, K. Wu, and G. Conciauro, "Dispersion characteristics of substrate integrated rectangular waveguide," *IEEE Microwave Wireless Components Letters*, Vol. 12, 333–335, 2002.
19. Hong, J. S. and M. J. Lancaster, *Microstrip Filter for RF/Microwave Applications,* Wiley, New York, 2001.
20. Zhou, C. X., Y. X. Guo, and S. L. Yan, "Efficient design of SIW filters with knowledge-embedded space mapping technique," *Journal of RF and Microwave Computer-Aided Engineering*, Vol. 22, No. 5, 603–609, 2012.